JOURNAL OF THE ROYAL SOCIETY Interface

rsif.royalsocietypublishing.org

Research

Cite this article: He F, Wang X, Maruyama O, Kosaka R, Sogo Y, Ito A, Ye J. 2013 Improvement in endothelial cell adhesion and retention under physiological shear stress using a laminin–apatite composite layer on titanium. J R Soc Interface 10: 20130014.
http://dx.doi.org/10.1098/rsif.2013.0014

Received: 8 January 2013
Accepted: 24 January 2013

Subject Areas:
biomaterials

Keywords:
titanium, apatite, laminin, endothelialization, cell adhesion, cell retention

Author for correspondence:
Xiupeng Wang
e-mail: xp-wang@aist.go.jp

Improvement in endothelial cell adhesion and retention under physiological shear stress using a laminin–apatite composite layer on titanium

Fupo He[1,2,3], Xiupeng Wang[1], Osamu Maruyama[3], Ryo Kosaka[3], Yu Sogo[1], Atsuo Ito[1] and Jiandong Ye[2,4]

[1]Human Technology Research Institute, National Institute of Advanced Industrial Science and Technology, Central 6, 1-1-1 Higashi, Tsukuba, Ibaraki 305-8566, Japan
[2]School of Materials Science and Engineering, South China University of Technology, Guangzhou 510641, People's Republic of China
[3]Human Technology Research Institute, National Institute of Advanced Industrial Science and Technology, Namiki1-2-1, Tsukuba, Ibaraki 305-8564, Japan
[4]National Engineering Research Center for Tissue Restoration and Reconstruction, Guangzhou 510006, People's Republic of China

Apatite (Ap), laminin–apatite composite (L5Ap, L10Ap, L20Ap and L40Ap) and albumin–apatite (AlbAp) composite layers were prepared on titanium (Ti) using a supersaturated calcium phosphate solution supplemented with laminin (0, 5, 10, 20 and 40 μg ml^{-1}) or albumin (800 μg ml^{-1}). With an increase in the concentrations of laminin in the supersaturated calcium phosphate solutions, the amounts of laminin immobilized on the Ti increased. The number of human umbilical vein endothelial cells (HUVECs) adhered to the laminin–apatite composite layers were remarkably higher than those to the untreated Ti, Ap layer and AlbAp composite layer. The number of cells adhered to the L40Ap was 4.3 times the untreated Ti. Moreover, cells adhered to the laminin–apatite composite layers showed significantly higher cell retention under the physiological shear stress for 1 h and 2 h than those to the untreated Ti, Ap layer and AlbAp composite layer. The number of cells remaining on the L40Ap under the physiological shear stress for 2 h was 9.5 times that of the untreated Ti. The laminin–apatite composite layer is a promising interfacial layer for endothelialization of blood-contacting materials.

1. Introduction

Antithrombogenicity is the first consideration for blood-contacting materials [1]. For example, although titanium (Ti) cardiac-assist devices exhibit favourable thromboresistance in short-term usage [2–4], they suffer from the risk of thrombogenesis in long-term usage [5]. Thromboresistance of Ti cardiac-assist devices has been improved by surface coating using 2-methacryloyloxyethyl phosphorylcholine polymer [6,7], TiO_2 [8], hydroxyapatite [9] and diamond-like carbon [10], and by surface-immobilized molecules including albumin [11], heparin [12], poly(ethylene glycol) [13] and chitosan [14]. Even today, however, most blood-contacting materials cause thrombogenesis in long-term usage.

Fast or prior endothelialization on the surface of the cardiac-assist devices is another promising strategy to inhibit thrombogenesis in long-term usage, as was indicated by earlier studies [15,16]. The formation of a monolayer of endothelial cells (ECs) on the material surface inhibits thrombogenesis by regulating coagulation cascade, the cellular components of the blood (leucocytes, platelets etc.) and complement cascade (vascular tone, fibrinolysis etc.) [17]. The challenges of endothelialization on the material surface are efficient cell adhesion, growth and retention under shear stress [18,19]. In addition, maintaining a confluent layer of healthy EC on the surface is an essential issue for long-term

Royal Society Publishing
Informing the science of the future

Table 1. Supersaturated calcium phosphate solutions.

total volume (ml)	×2.0 Ringer's (ml)	×2.0 Ringer's-laminin (ml)	×2.0 Ringer's-albumin (ml)	×2.0 Klinisalz B (ml)	Alkalinizer (ml)
3	1.25–2.45	0–1.20	0–0.48	0.28	0.27

application of cardiac-assist devices. In this context, it should be noted that as high as 30 per cent of cells detached from well-endothelialized vascular prostheses in 30 min after implantation in dogs [18]. Therefore, improvement in bonding strength between ECs and Ti surface is crucial for the development of endothelialized Ti that has a long-term antithrombogenic property.

Surface modification of biomaterials with adhesive peptide sequences has been proposed to improve EC adhesion, spreading and retention under the shear stress [20–24]. Laminin, which is the major adhesive glycoprotein in the basement membrane, can promote cell adhesion and be involved in cell migration, proliferation and differentiation [25–27]. However, the biomolecules are highly susceptive to physiological diffusion and degradation processes, leading to a short half-life [28,29]. Ap is a promising matrix for biomolecules to maintain their bioactivity and to induce persistent signalling [30–37]. Besides, Ap, as the main inorganic component of human hard tissues, has good biocompatibility and has been reported to show good thromboresistance [9]. In the present study, a laminin–apatite composite layer was prepared on Ti to improve *in vitro* EC adhesion and retention.

2. Material and methods

2.1. Preparation of Ti specimens

Commercially available Ti plate (Nilaco Co., Japan) was cut into square pieces of $10 \times 10 \times 1\ mm^3$ using a boron carbide blade (RCA 005, Refine Saw). The Ti plates were ultrasonically washed with acetone, ethanol and ultrapure water for 30 min. After being washed, the Ti plates were heated at 300°C for 3 h in air. The heat-treated Ti was then sterilized at 150°C for 2 h before being coated with Ap, albumin–apatite (AlbAp) composite and laminin–apatite composite layers.

2.2. Preparation of supersaturated calcium phosphate solutions

A calcium-containing solution (4.5 mM Ca^{2+}, ×2.0 Ringer's) was obtained by mixing Ringer's solution (Otsuka Pharmaceutical Co., Ltd, Japan, 2.25 mM Ca^{2+}) and Conclyte-Ca (Otsuka Pharmaceutical Co., Ltd, 500 mM Ca^{2+}). Laminin solution at a concentration of 100 μg ml^{-1} (2.0 Ringer's-laminin) and albumin solution at a concentration of 5 mg ml^{-1} (2.0 Ringer's-albumin) were prepared by dissolving laminin (Sigma-Aldrich, USA) and albumin (Invitrogen, USA) in the calcium-containing solution (4.5 mM Ca^{2+}, ×2.0 Ringer's). A phosphate-containing solution (20 mM PO_4^{3-}, ×2.0 Klinisalz B) was obtained by mixing Klinisalz B (I'rom Pharmaceutical Co., Ltd, Japan, 10 mM PO_4^{3-}) and Conclyte solution-PK (Otsuka Pharmaceutical Co., Ltd, Japan, 500 mM PO_4^{3-}). An alkalinizer Bifil (Ajinomoto Pharmaceuticals Co., Ltd, Japan, 166 mM $NaHCO_3$) was used as received without changing its original concentration. All the solutions used in this study were infusion fluids clinically available in Japan. The merits of using clinically approved pharmaceutical formulations are that they are sterile and endotoxin-free, and have a low regulatory barrier for clinical applications [30–35].

2.3. Formation of apatite, laminin–apatite composite and albumin–apatite composite layers on Ti plates

The sterilized Ti plates were immersed in 3 ml of supersaturated calcium phosphate solution supplemented with albumin or laminin solution at the mixing ratio shown in table 1, at 37°C for 48 h. The chemical compositions of the supersaturated calcium phosphate solutions used are shown in table 2. The Ti plates immersed in the supersaturated calcium phosphate solutions are designated as Ap, L5Ap, L10Ap, L20Ap, L40Ap and AlbAp depending on laminin or albumin concentrations as shown in table 2. After immersion, the Ti plates were taken out from the solution and gently washed twice by immersing in 10 ml of sterilized ultrapure water.

2.4. Quantitative analysis of calcium, phosphorus, laminin, and albumin in apatite, laminin–apatite composite and albumin–apatite composite layers

The coated Ti plates were immersed in 3 ml of 0.4 M hydrochloric acid solution at room temperature for 12 h to extract the calcium, phosphorus, laminin and albumin completely by dissolving the layers. The calcium and phosphorus were measured using an inductively coupled plasma atomic emission spectrometer (SPS7800, Seiko Instruments, Inc., Japan). The amounts of laminin and albumin in the hydrochloric acid solution were measured using a Bio-Rad protein assay reagent kit (Bio-Rad Laboratories, Inc., Japan) in accordance with the manufacturer's instructions.

2.5. Characterization of the apatite, laminin–apatite composite and albumin–apatite composite layers

The surface morphology of the layers on the Ti plates was observed under a scanning electron microscope (SEM: XL30, FEI Company Ltd) at an accelerating voltage of 10 kV after being coated with gold. The phase composition of the Ap, laminin–apatite composite and AlbAp composite layers were analysed by thin-film X-ray diffractometry (TF-XRD) employing a Cu Kα X-ray at 40 kV and 300 mA using a thin-film X-ray diffractometer (Model RINT 2400, Rigaku, Japan).

2.6. Adhesion of human umbilical vein endothelial cells to Ti, Ap, L5Ap, L10Ap, L20Ap, L40Ap and AlbAp

A 1.0 ml bolus of serum-free EC basal medium-2 (EBM-2, Lonza, USA) containing 2×10^4 human umbilical vein endothelial cells (HUVECs) was added onto the Ti, Ap, L5Ap, L10Ap, L20Ap, L40Ap and AlbAp specimens in wells of a 24-well cell culture plate. After being incubated in a humidified atmosphere of 5 per cent CO_2 at 37°C for 1 h, the specimens were gently rinsed with phosphate-buffered saline (PBS(−)) twice. The specimens seeded with HUVECs were then transferred to the wells of a new 24-well plate with 1 ml of fresh serum-free EBM-2 supplemented with 2 μM cell tracker green 5-chloromethyl fluorescence diacetate (CTG, Invitrogen, USA) agent. The CTG agent was used to stain the HUVECs adhered to the surface of

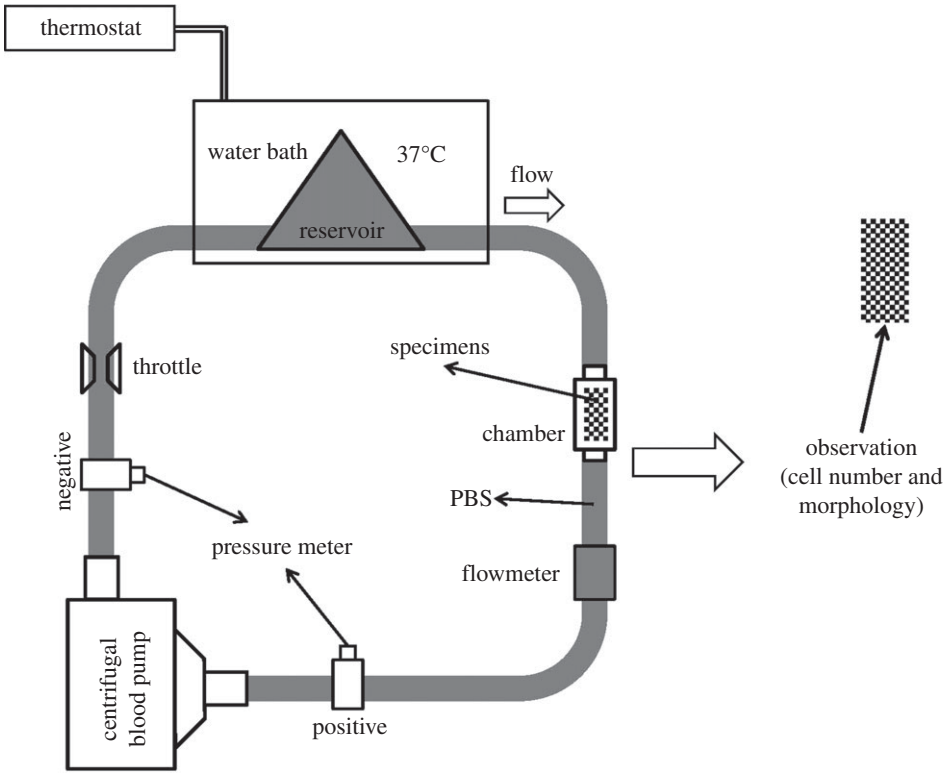

Figure 1. Scheme of *in vitro* HUVECs retention evaluation system (HUVECs were subjected to physiological shear stress then observed using a fluorescence microscope).

Table 2. Chemical components of supersaturated calcium phosphate solutions.

components	Ap	L5Ap	L10Ap	L20Ap	L40Ap	AlbAp
Na^+ (mM)	138.75	138.75	138.75	138.75	138.75	138.75
K^+ (mM)	7.37	7.37	7.37	7.37	7.37	7.37
Ca^{2+} (mM)	3.68	3.68	3.68	3.68	3.68	3.68
Mg^{2+} (mM)	0.22	0.22	0.22	0.22	0.22	0.22
Cl^- (mM)	134.27	134.27	134.27	134.27	134.27	134.27
$H_2PO_4^-$ (mM)	0.90	0.90	0.90	0.90	0.90	0.90
HPO_4^{2-} (mM)	0.94	0.94	0.94	0.94	0.94	0.94
HCO_3^- (mM)	15.09	15.09	15.09	15.09	15.09	15.09
CH_3COO^- (mM)	1.80	1.80	1.80	1.80	1.80	1.80
laminin (μg/ml)	0	5	10	20	40	0
albumin (μg/ml)	0	0	0	0	0	800

specimens. After incubation in a humidified atmosphere of 5 per cent CO_2 at 37°C for 45 min, the specimens were gently washed with PBS to remove the residual CTG agent. The cells adhered to the specimens were observed under a fluorescence microscope (BX51, Olympus, Japan). For each specimen, 20 pictures from different samples were taken to count the number of HUVECs adhered to the specimen surface.

2.7. Cell retention under the physiological shear stress

An *in vitro* circulation system was used to assess the retention of HUVECs adhered to the specimens under the physiological shear stress. As shown in figure 1, the *in vitro* circulation system consisted of a reservoir (Senko Medical Instrument Mfg. Co., Japan) containing PBS(−) solution, a centrifugal blood pump (HCF-MP23, Senko Medical Instrument Mfg. Co., Japan) and a special chamber holding the specimens seeded with HUVECs connected by polyvinyl chloride tubing (Senko Medical Instrument Mfg. Co., Japan) [38]. Prior to the cell retention study, 1×10^5 HUVECs were seeded on the specimens and cultured by EBM-2 with serum in a humidified atmosphere of 5 per cent CO_2 at 37°C for one week. The cell culture medium was exchanged for a fresh one every 2 days. The cells were stained with CTG agent and observed under a fluorescence microscope. Then the specimens seeded with HUVECs were put in the special chamber of the *in vitro* circulation system to study cell retention on the Ti, Ap, AlbAp and L40Ap under physiological shear stress. The working parameters of the *in vitro* circulation system were as follows: pressure, 190 mm Hg; flow rate, 4 l min^{-1} (shear stress at tube wall, 0.7 Pa); temperature, 37°C. After 1 h and 2 h exposure to the physiological shear stress, the retained cells on the specimens were observed under a fluorescence microscope. Cell retention on the specimen surfaces was evaluated by comparing the cell numbers before and after being subjected to the physiological shear stress.

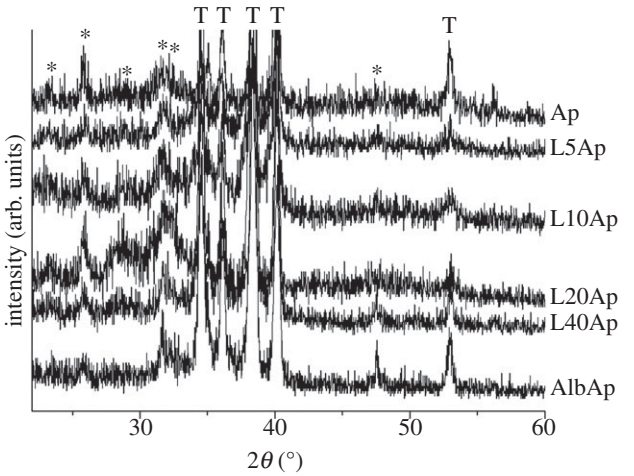

Figure 2. XRD patterns of Ap, L5Ap, L10Ap, L20Ap, L40Ap and AlbAp on Ti. An asterisk denotes apatite and a T denotes titanium.

2.8. Data analysis

Statistical comparisons were performed by Student's *t*-test for multiple comparisons. Statistical significance for $p < 0.05$ and $p < 0.01$ were denoted by one and two asterisks respectively.

3. Results

3.1. Phase composition and surface morphology of apatite, laminin–apatite composite and albumin–apatite composite layers

The XRD patterns for Ap, laminin–apatite composite and AlbAp composite layers on Ti are shown in figure 2. Weak and broad peaks were present at 25.8° and 31.8° (ICDD NO. 09-432), which denoted that the layers on the Ti were composed of poorly crystalline Ap.

The surface morphology of Ap, laminin–apatite composite and AlbAp composite layers on the Ti is shown in figure 3. The Ti without immersion in the supersaturated calcium phosphate solution exhibited a smooth surface (figure 3, Ti). After immersing in the supersaturated calcium phosphate solutions at 37°C for 48 h, continuous and homogeneous layers were formed on the whole Ti surface. The layers were composed of fine flake-like crystals, with thickness of about 20 nm and length of 200 nm, which have been identified as poorly crystalline Ap (figure 2). The laminin–apatite composite and AlbAp composite layers exhibited structure similar to Ap layer.

3.2. Chemical compositions of apatite, laminin–apatite composite and albumin–apatite composite layers

The amount of Ap deposited on the Ti surfaces was assessed by measuring the amounts of calcium (Ca) and phosphorus (P) after dissolution of Ap, laminin–apatite composite and AlbAp composite layers. As shown in figure 4, compared to Ap, the L5Ap, L10Ap, L20Ap and L40Ap prepared by immersion in the supersaturated calcium phosphate solution supplemented with various concentrations of laminin (5, 10, 20 and 40 $\mu g\ ml^{-1}$) showed no obvious difference in calcium and phosphorus deposition (calcium, from 38.46 ± 6.40 to 42.86 ± 8.10 μg/sample; phosphorus, from 16.73 ± 2.42 to 19.01 ± 3.23 μg/sample). However, with regard to AlbAp prepared by immersion in the supersaturated calcium phosphate solution containing 800 $\mu g\ ml^{-1}$ albumin, the calcium and phosphorus deposited on the Ti significantly decreased (calcium, 23.02 ± 7.34; phosphorus, 10.45 ± 2.86) by comparison with Ap.

Figure 5 shows the amounts of laminin and albumin coprecipitated with Ap on the Ti surface. The amounts of laminin precipitated on the Ti surface increased with an increase in initial laminin concentration in the supersaturated calcium phosphate solution. When the laminin concentration in the solution was 5, 10, 20 and 40 $\mu g\ ml^{-1}$, the amount of laminin precipitated on Ti surfaces was 0.79 ± 0.61, 2.78 ± 1.35, 8.39 ± 3.84 and 20.69 ± 3.71 μg/sample, respectively. The amount of albumin precipitated on the Ti surface was 81.70 ± 24.59 μg/sample.

3.3. Effect of apatite, laminin–apatite composite and albumin–apatite composite layers on human umbilical vein endothelial cells adhesion

Figure 6*a* shows typical fluorescent images of HUVECs adhered to the surfaces of Ti, Ap, L5Ap, L10Ap, L20Ap, L40Ap and AlbAp specimens after being cultured for 1 h. The HUVECs adhered to the specimen surfaces were spherical. The stretched pseudopodia were observed on the cells adhered to the surface of L20Ap (data not shown) and L40Ap (figure 6*a*, L40Ap-H). However, no obvious pseudopodia were observed on the cells adhered to untreated Ti, Ap and AlbAp (figure 6*a*, Ti-H, Ap-H and AlbAp-H). The numbers of HUVECs adhered to the surfaces of the Ti, Ap, L5Ap, L10Ap, L20Ap, L40Ap and AlbAp specimens after 1 h of culture are shown in figure 6*b*. The number of cells adhered to the Ap was slightly larger than that to the untreated Ti. AlbAp showed slightly more cell adhesion than untreated Ti and Ap. The number of cells adhered to the surfaces of L5Ap, L10Ap, L20Ap, L40Ap was markedly higher than that to the untreated Ti, Ap and AlbAp. The number of cells adhered to the surfaces of laminin–apatite composite layer increased with an increase in amount of laminin precipitated on the Ti surface (0–40 $\mu g\ ml^{-1}$). The number of cells adhered to the L40Ap reached the maximum value of $2.3 \times 10^3\ cm^{-2}$, which was 4.3 times as large as the untreated Ti. Based on the cell adhesion results, Ti, Ap, AlbAp and L40Ap were selected for the following cell retention test.

3.4. Human umbilical vein endothelial cells retention under the physiological shear stress

Cell retention on the surfaces of Ti, Ap, AlbAp and L40Ap specimens was studied using an *in vitro* circulation system producing a physiological shear stress of 0.7 Pa, which corresponded to that in the human blood vessels. Typical fluorescent images of HUVECs adhered to the Ti, Ap, AlbAp and L40Ap specimens before and after exposure to the physiological shear stress are shown in figure 7*a*. After being subjected to the physiological shear stress for 1 h, significant cell detachment was observed on the surfaces of Ti, Ap and AlbAp, while only a small amount of cell detachment was observed on the L40Ap. After the specimens had been exposed to the physiological shear stress for 2 h, most of the cells had detached from the Ti, Ap and AlbAp surfaces, but most cells remained on the L40Ap surface. The number and percentage of cell retention on the specimens are

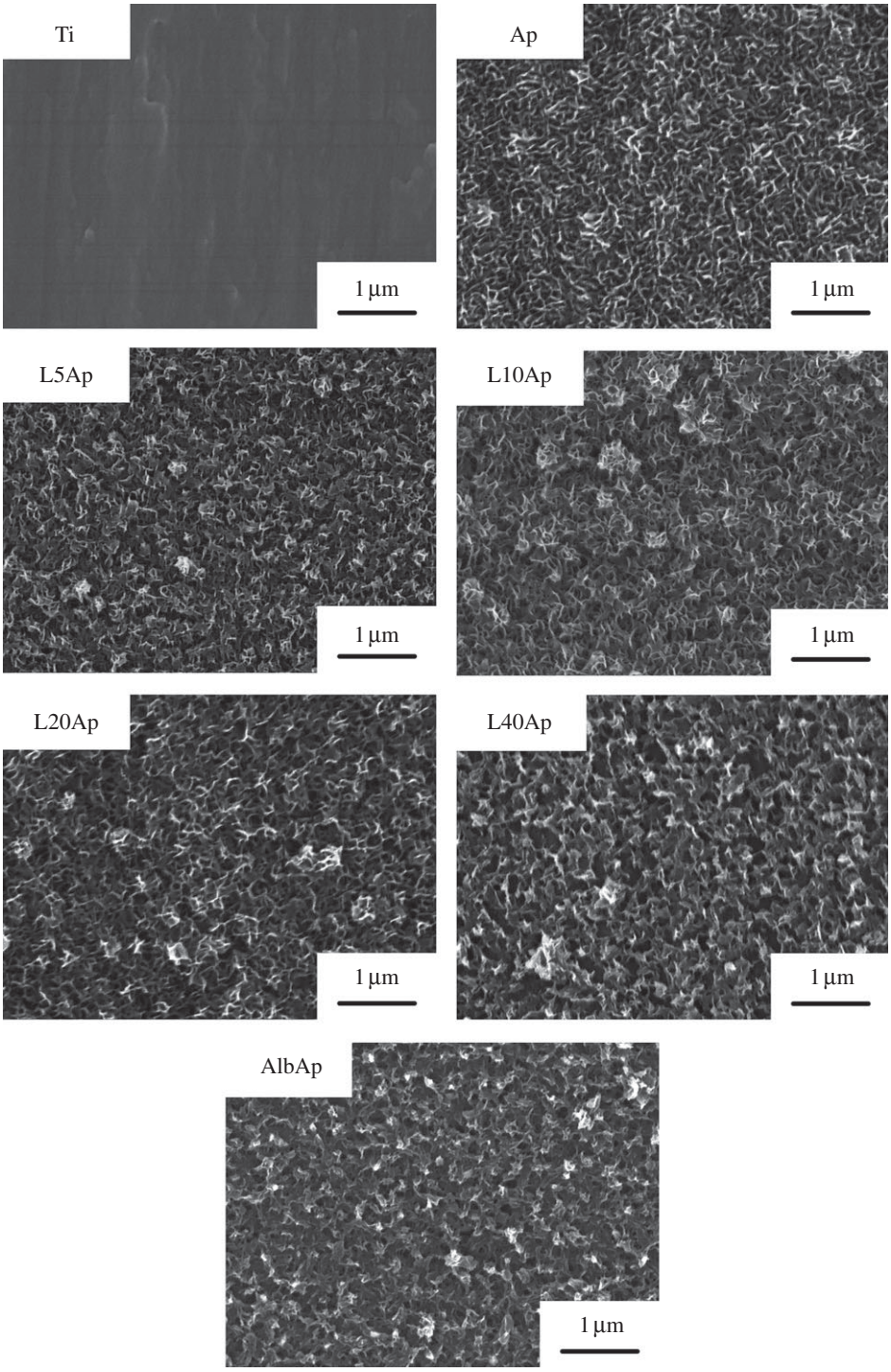

Figure 3. SEM images of Ti, Ap, L5Ap, L10Ap, L20Ap, L40Ap and AlbAp.

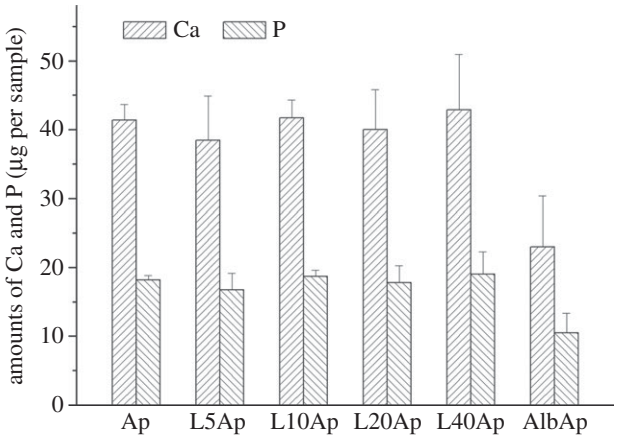

Figure 4. Amounts of calcium and phosphorus precipitated on Ti.

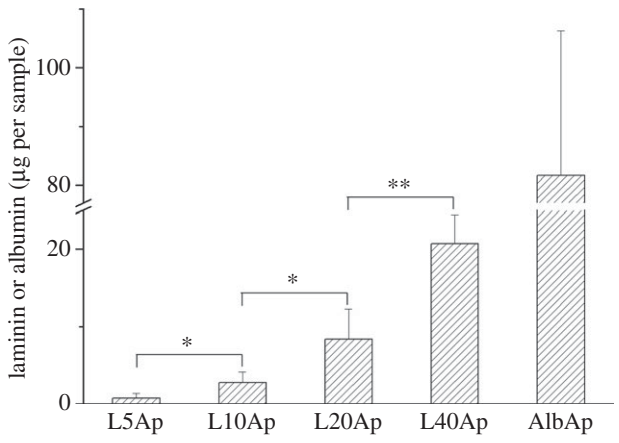

Figure 5. Amounts of laminin or albumin precipitated on Ti.

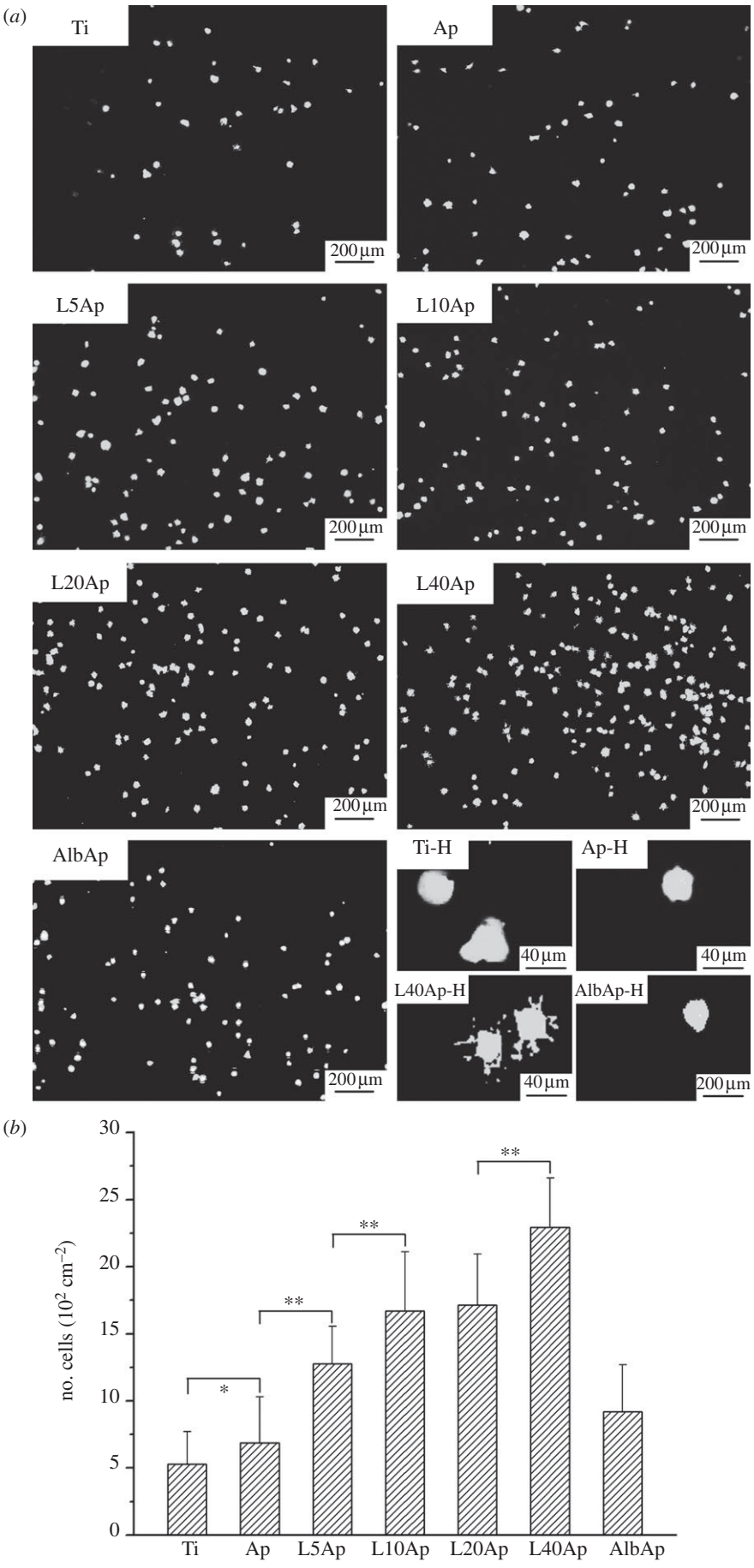

Figure 6. (*a*) Fluorescent images of HUVECs adhered to Ti, Ap, L5Ap, L10Ap, L20Ap, L40Ap and AlbAp after being cultured for 1 h (Ti-H, Ap-H, L40Ap-H and AlbAp-H are images of HUVECs adhered to the surfaces of Ti, Ap, L40Ap and AlbAp under higher magnification, respectively). (*b*) Numbers of HUVECs adhered to the surfaces of Ti, Ap, L40Ap and AlbAp after being cultured for 1 h.

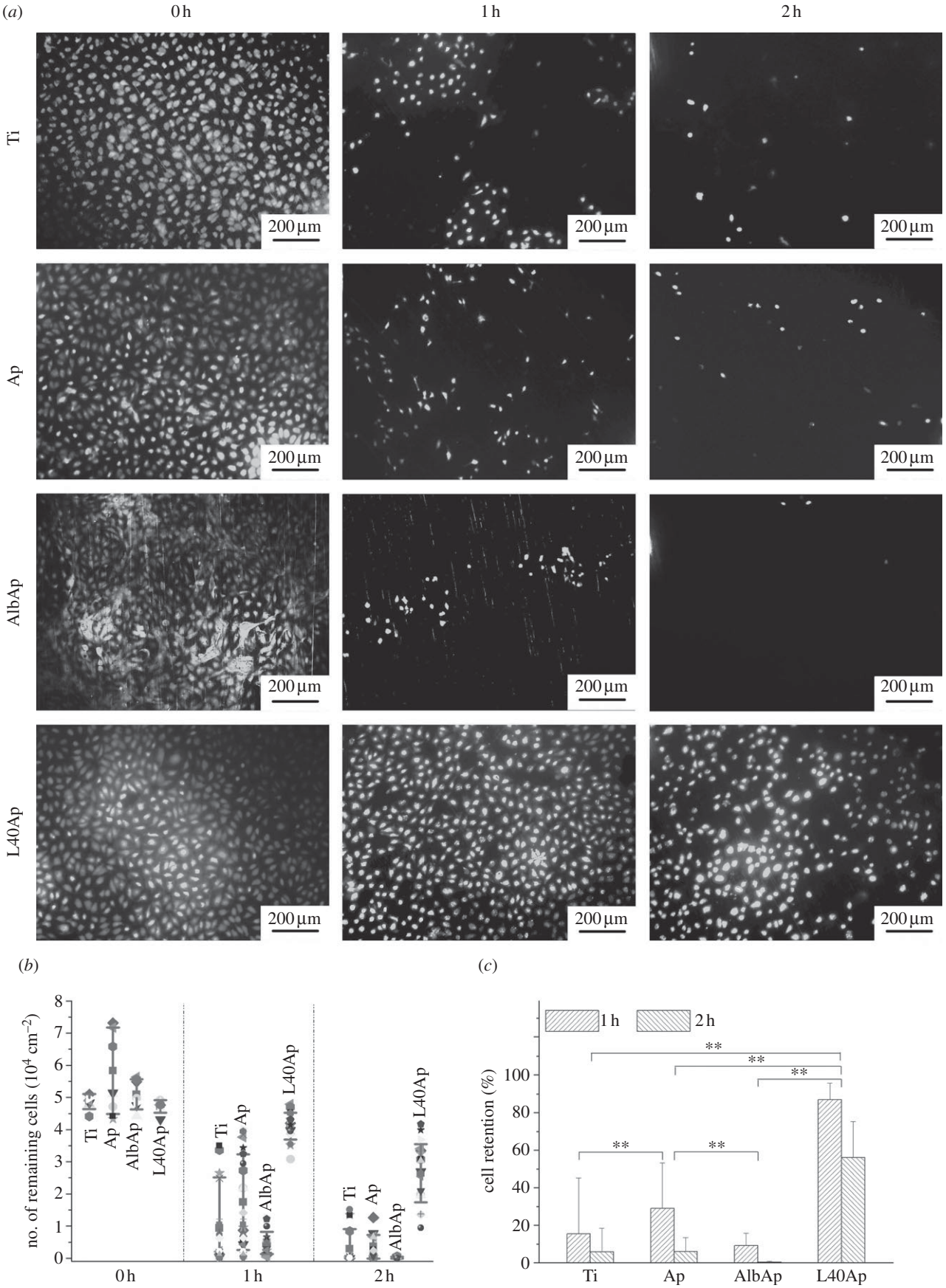

Figure 7. (*a*) Fluorescent images of HUVECs adhered to Ti, Ap, L40Ap and AlbAp after being subjected to physiological shear stress for 0, 1 and 2 h. (*b*) Number of and (*c*) percentage of cells remaining on the Ti, Ap, L40Ap and AlbAp after being subjected to physiological shear stress for 0, 1 and 2 h.

shown in figure 7*b*,*c*, respectively. The cell retention on L40Ap was significantly higher than those on Ti, Ap and AlbAp. After exposure to physiological shear stress for 1 h, the percentage of cell retention on the Ti, Ap, AlbAp and L40Ap was 15.47 ± 29.74%, 29.11 ± 24.16%, 9.21 ± 6.67% and 87.02 ± 8.76%, respectively. After 2 h, cell retention on the Ti, Ap, AlbAp and L40Ap decreased to 5.88 ± 12.55%, 6.10 ± 7.32%, 0.31 ± 0.58% and 56.04 ± 19.18%, respectively. After evaluation of cell retention under flow conditions, the coatings (Ap, L5Ap, L10Ap, L20Ap, L40Ap

and AlbAp) still homogeneously covered the surface of Ti as observed by SEM. The morphology of coatings (Ap, LAp etc.) before and after flow conditions were almost same as observed by SEM (data not shown). The coating strength is enough for the flow conditions.

4. Discussion

Laminin–apatite composite layers were prepared on the Ti surface. HUVECs adhering to the laminin–apatite composite layers after 1 h of culture (4.3 times maximum), and remaining under physiological shear stress for 2 h (9.5 times maximum), were significantly higher than those on untreated Ti, Ap and AlbAp composite layers.

Ap, laminin–apatite composite and AlbAp composite layers were successfully formed on the commercially available Ti plates by using a metastable supersaturated calcium phosphate solution supplemented with laminin and albumin. Low-crystalline Ap was formed by consuming calcium and phosphate ions in the supersaturated calcium phosphate solutions. The carboxyl and hydroxyl groups of the laminin or albumin molecule can bind to the calcium ions in the solutions and on the growing calcium phosphate [39]. The amounts of laminin precipitated in the Ap increased with increasing laminin concentration in the supersaturated calcium phosphate solution (figure 5). The albumin incorporated into the crystal lattice of Ap enhanced the layer's hardness and resistance to abrasion [40]. The laminin immobilized in the Ap layer increased the shear stress of layer under the wet condition [41].

Cell adhesion is the first step reaction at HUVECs-biomaterial interface, which is followed by cell migration, proliferation and final endothelialization. Cell adhesion plays an important role in fast endothelialization of biomaterial surface. Adhesion of mammalian cells to a biomaterial surface is mediated by a protein layer from biological fluids or extracellular matrix so that the cell first interacts with protein when contacting with biomaterial surface [42]. Moreover, the cell adhesion is regulated and mediated by membrane proteins with a main family being integrins which present a very high selectivity towards the extracellular matrix proteins [42]. Laminin has been found to interact with at least eight integrins (α1β1, α2β1, α3β1, α6β1, α7β1, α9β1, $\alpha_V\beta3$ and α6β4). Therefore, laminin can promote adhesion of diverse cells by interacting with integrin and non-integrin receptors on the cell surface [43,44]. α6β1 and α6β4 integrins, which are present in the EC surface, are the main laminin receptors [45]. The integrin α6β1 plays an important role in mediating adhesion of EC to the laminin [46], while α6β4 supports the effect of laminin on modulation of EC function relevant to angiogenesis [45]. Therefore, the number of HUVECs adhering to the surface of laminin–apatite composite layers increased with the increasing amount of laminin incorporated in the Ap on the Ti surface.

The retention of HUVECs on the artificial cardiovascular materials under the physiological shear stress is a crucial index for long-term usage. The major issue of endothelialization on biomaterial surfaces is low retention of HUVECs under fluid shear stress [18,19]. Pratt *et al*. [47] reported that cells not tightly adhered to the material surface were easily washed away when exposed to fluid shear stress. Therefore, the cell–material reaction was the main factor that affected cell adhesion under shear stress. We evaluated the cell retention on the surfaces of Ti, Ap, AlbAp and L40Ap under the physiological shear stress, which was generated by an *in vitro* circulation system with a centrifugal blood pump. HUVECs were subjected to the shear stress at 0.7 Pa for 1 and 2 h, respectively. A mass of cells on the Ti were removed under the physiological shear stress due to lacking in functional groups on the Ti to interact with HUVECs. The L40Ap displayed markedly improved cell retention under physiological shear stress, compared to untreated Ti, Ap, and AlbAp. The laminin played a major role in the promotion of shear stability of HUVECs, which may be attributed to mediation of laminin on cellular activity. In this study, we focused on preparing the EC layer *in vitro* and evaluating cell adhesion and retention *in vitro*. This technique may also be interesting for forming EC layers *in vivo*. Therefore, in future work, dynamic cell seeding techniques *in vitro* will be used to mimic *in situ* endothelialization before *in vivo* study.

5. Conclusions

Ap, laminin–apatite composite and AlbAp composite layers were prepared on the Ti surface by supersaturated calcium phosphate solutions supplemented with laminin and albumin, respectively. Supplementing laminin did not obviously influence the amount of Ap deposited on the Ti surface. The amounts of laminin precipitated in the laminin–apatite composite layers increased with increasing initial laminin concentration in the supersaturated calcium phosphate solution. The number of cells adhered to the laminin–apatite composite layers were significantly higher than those to the untreated Ti, Ap layer and AlbAp composite layer. Moreover, cells remaining on the laminin–apatite composite layer under physiological shear stress for 1 and 2 h were significantly higher than those on untreated Ti, Ap and AlbAp composite layers. Cells on L40Ap showed 4.3 times greater adhesion after 1 h of culture and 9.5 times greater retention under physiological shear stress for 2 h than those on untreated Ti. The laminin–apatite composite layer can be used for endothelialization of blood-contacting materials.

F.H. received a China Scholarship Council (CSC) scholarship (2011615041).

References

1. Balasubramanian V, Hall CL, Shivashankar S, Slack SM, Turitto VT. 1998 Vascular cell attachment and procoagulant activity on metal alloys. *J. Biomater. Sci. Polym. Ed.* **9**, 1349–1359. (doi:10.1163/156856298X00433)
2. McCarthy PM, Smith WA. 2002 Mechanical circulatory support—a long and winding road. *Science* **295**, 998–999. (doi:10.1126/science.1068555)
3. Takami Y, Yamane S, Makinouchi K, Niimi Y, Sueoka A, Nose Y. 1998 Evaluation of platelet adhesion and

activation on materials for an implantable centrifugal blood pump. *Artif. Organs.* **22**, 753–758. (doi:10.1046/j.1525-1594.1998.6184R.x)

4. Dion I, Baquey C, Monties JR, Havlik P. 1993 Haemocompatibility of Ti6A14V alloy. *Biomaterials* **14**, 122–126. (doi:10.1016/0142-9612(93)90222-N)
5. Achneck HE, Sileshi B, Parikh A, Milano CA, Welsby IJ, Lawson JH. 2010 Pathophysiology of bleeding and clotting in the cardiac surgery patient: from vascular endothelium to circulatory assist device surface. *Circulation* **122**, 2068–2077. (doi:10.1161/CIRCULATIONAHA.110.936773)
6. Ye SH, Johnson Jr CA, Woolley JR, Murata H, Gamble LJ, Ishihara K, Wangner WR. 2010 Simple surface modification of a titanium alloy with silanated zwitterionic phosphorylcholine or sulfobetaine modifiers to reduce thrombogenicity. *Colloids. Surf. B* **79**, 357–364. (doi:10.1016/j.colsurfb.2010.04.018)
7. Sin DC, Kei HL, Miao X. 2009 Surface coatings for ventricular assist devices. *Expert. Rev. Med. Devices.* **6**, 51–60. (doi:10.1586/17434440.6.1.51)
8. Huang N *et al*. 2003 Hemocompatibility of titanium oxide films. *Biomaterials* **24**, 2177–2187. (doi:10.1016/S0142-9612(03)00046-2)
9. Muramatsu K, Uchida M, Kim HM, Fujisawa A, Kokubo T. 2003 Thromboresistance of alkali- and heat-treated titanium metal formed with apatite. *J. Biomed. Mater. Res. Part A* **65**, 409–416. (doi:10.1002/jbm.a.10494)
10. Hasebe T *et al*. 2006 Fluorinated diamond-like carbon as antithrombogenic coating for blood-contacting devices. *J. Biomed. Mater. Res. Part A* **76**, 86–94. (doi:10.1002/jbm.a.30512)
11. Uchida M *et al*. 2005 Reduced platelet adhesion to titanium metal coated with apatite, albumin-apatite composite or laminin-apatite composite. *Biomaterials* **26**, 6924–6931. (doi:10.1016/j.biomaterials.2005.04.066)
12. Gong FR, Cheng XY, Wang SF, Zhao YC, Gao Y, Cai HB. 2010 Heparin-immobilized polymers as non-inflammatory and non-thrombogenic coating materials for arsenic trioxide eluting stents. *Acta Biomater.* **6**, 534–546. (doi:10.1016/j.actbio.2009.07.013)
13. Tanaka Y, Matsuo Y, Komiya T, Tsutsumi Y, Doi H, Yoneyama T, Hanawa T. 2010 Characterization of the spatial immobilization manner of poly(ethylene glycol) to a titanium surface with immersion and electrodeposition and its effects on platelet adhesion. *J. Biomed. Mater. Res. Part A* **92**, 350–358. (doi:10.1002/jbm.a.32375)
14. Luo LL, Wang GX, Li YL, Yin TY, Jiang T, Ruan CG. 2011 Layer-by-layer assembly of chitosan and platelet monoclonal antibody to improve biocompatibility and release character of PLLA coated stent. *J. Biomed. Mater. Res. Part A* **97**, 423–432. (doi:10.1002/jbm.a.33066)
15. Ortenwall P, Wadenvik H, Kutti J, Risberg B. 1987 Reduction in deposition of indium 111 labelled platelets after autologous endothelial cell seeding of Dacron aortic bifurcation grafts in humans: a preliminary report. *J. Vasc. Surg.* **6**, 17–25. (doi:10.1067/mva.1987.avs0060017)
16. Graham LM, Burkel WE, Ford JW, Vinter DW, Kahn RH, Stanley JC. 1980 Immediate seeding of enzymatically derived endothelium in Dacron vascular grafts. Early experimental studies with autologous canine cells. *Arch. Surg.* **115**, 1289–1294. (doi:10.1001/archsurg.1980.01380110033005)
17. McGuigan AP, Sefton MV. 2007 The influence of biomaterials on endothelial cell thrombogenicity. *Biomaterials* **28**, 2547–2571. (doi:10.1016/j.biomaterials.2007.01.039)
18. Rosenman JE, Kempczinski RF, Pearce WH, Silberstein EB. 1985 Kinetics of endothelial cell seeding. *J. Vasc. Surg.* **2**, 778–784. (doi:10.1067/mva.1985.avs0020778)
19. Fields C, Cassano A, Allen C, Meyer A, Pawlowski KJ, Bowlin GL, Rittgers SE, Szycher M. 2002 Endothelial cell seeding of a 4-mm I.D. polyurethane vascular graft. *J. Biomater. Appl.* **17**, 45–70. (doi:10.1106/088532802027861)
20. Jun HW, West JL. 2005 Modification of polyurethaneurea with PEG and YIGSR peptide to enhance endothelialization without platelet adhesion. *J. Biomed. Mater. Res. Part B* **72**, 131–139. (doi:10.1002/jbm.b.30135)
21. Holland J, Hersh L, Bryhan M, Onyiriuka E, Ziegler L. 1996 Culture of human vascular endothelial cells on an RGD-containing synthetic peptide attached to a starch-coated polystyrene surface: comparison with fibronectin-coated tissue grade polystyrene. *Biomaterials* **17**, 2147–2156. (doi:10.1016/0142-9612(96)00028-2)
22. Jun H, West J. 2004 Development of a YIGSR-peptide-modified polyurethaneurea to enhance endothelialization. *J. Biomater. Sci. Polym. Ed.* **15**, 73–94. (doi:10.1163/156856204322752246)
23. Larsen CC, Kligman F, Tang C, Marchanta KK, Marchant RE. 2007 A blomimetic peptide fluorosurfactant polymer for endothelialization of ePTFE with limited platelet adhesion. *Biomaterials* **28**, 3537–3548. (doi:10.1016/j.biomaterials.2007.04.026)
24. Tiwari A, Salacinski HJ, Punshon G, Hamilton G, Seifalian AM. 2002 Development of a hybrid cardiovascular graft using a tissue engineering approach. *FASEB. J.* **16**, 791–796. (doi:10.1096/fj.01-0826com)
25. Malinda KM, Kleinman HK. 1996 The laminins. *Int. J. Biochem. Cell. Biol.* **9**, 957–959. (doi:10.1016/1357-2725(96)00042-8)
26. Engbring JA, Kleinman HK. 2003 The basement membrane matrix in malignancy. *J. Pathol.* **200**, 465–470. (doi:10.1002/path.1396)
27. Nomizu M *et al*. 1998 Cell binding sequences in mouse laminin α1 chain. *J. Biol. Chem.* **273**, 32 491–32 499. (doi:10.1074/jbc.273.49.32491)
28. Sellers RS, Zhang R, Glasson SS, Kim HD, Peluso D, D'Augusta DA, Beckwith K, Morris EA. 2000 Repair of articular cartilage defects one year after treatment with recombinant human bone morphogenetic protein-2 (rhBMP-2). *J. Bone. Joint. Surg. Am.* **82**, 151–160.
29. Bonadio J. 2000 Tissue engineering via local gene delivery: update and future prospects for enhancing the technology. *Adv. Drug. Deliv. Rev.* **44**, 185–194. (doi:10.1016/S0169-409X(00)00094-6)
30. Wang XP, Li X, Onuma K, Ito A, Sogo Y, Kosuge K, Oyane A. 2010 Mesoporous bioactive glass coatings on stainless steel for enhanced cell activity, cytoskeletal organization and AsMg immobilization. *J. Mater. Chem.* **20**, 6437–6445. (doi:10.1039/c0jm00399a)
31. Li X, Wang XP, Ito A, Sogo Y, Cheng K, Oyane A. 2009 Effect of coprecipitation temperature on the properties and activity of fibroblast growth factor-2 apatite composite layer. *Mater. Sci. Eng. C* **29**, 216–221. (doi:10.1016/j.msec.2008.06.012)
32. Wang XP, Ito A, Sogo Y, Li X, Tsurushima H, Oyane A. 2009 Ascorbate-apatite composite and ascorbate-FGF-2-apatite composite layers formed on external fixation rods and their effects on cell activity *in vitro*. *Acta Biomater.* **5**, 2647–2656. (doi:10.1016/j.actbio.2009.03.020)
33. Wang XP, Ito A, Sogo Y, Li X, Oyane A. 2010 Zinc-containing apatite layers on external fixation rods promoting cell activity. *Acta Biomater.* **6**, 962–968. (doi:10.1016/j.actbio.2009.08.038)
34. Wang XP, Ito A, Sogo Y, Li X, Oyane A. 2010 Silicate-apatite composite layers on external fixation rods and *in vitro* evaluation using fibroblast and osteoblast. *J. Biomed. Mater. Res. Part A* **92**, 1181–1189. (doi:10.1002/jbm.a.32436)
35. Wang X, Ito A, Li X, Sogo Y, Oyane A. 2011 Signal molecules-calcium phosphate coprecipitation and its biomedical application as a functional coating. *Biofabrication* **3**, 022001. (doi:10.1088/1758-5082/3/2/022001)
36. Oyane A, Wang XP, Sogo Y, Ito A, Tsurushima H. 2012 Calcium phosphate composite layers for surface-mediated gene transfer. *Acta Biomater.* **8**, 2034–2046. (doi:10.1016/j.actbio.2012.02.003)
37. Wang XP, Oyane A, Tsurushima H, Sogo Y, Li X, Ito A. 2011 BMP-2 and ALP gene expression induced by a BMP-2 gene-fibronectin-apatite composite layer. *Biomed. Mater.* **6**, 045004. (doi:10.1088/1748-6041/6/4/045004)
38. Maruyama O, Tomari Y, Sugiyama D, Nishida M, Tsutsui T, Yamane T. 2009 Simple *in vitro* testing method for antithrombogenic evaluation of centrifugal blood pumps. *ASAIO. J.* **55**, 314–322. (doi:10.1097/MAT.0b013e3181a7b540)
39. Oyane A, Uchida M, Onuma K, Ito A. 2006 Spontaneous growth of a laminin-apatite nano-composite in a metastable calcium phosphate solution. *Biomaterials* **27**, 167–175. (doi:10.1016/j.biomaterials.2005.06.001)
40. Liu Y, Hunziker EB, Randall NX, de Groot K, Layrolle P. 2003 Proteins incorporated into biomimetically prepared calcium phosphate coatings modulate their mechanical strength and dissolution rate. *Biomaterials* **24**, 65–70. (doi:10.1016/S0142-9612(02)00252-1)
41. Oyane A, Yokoyama Y, Kasahara M, Ichinose N, Saito M, Ito A. 2009 Mechanical properties of a laminin-apatite composite layer formed on an ethylene-

vinyl alcohol copolymer. *Mater. Sci. Eng. C* **29**, 1681–1686. (doi:10.1016/j.msec.2009.01.012)
42. Ponche A, Ploux L, Anselme K. 2010 Protein/material interfaces: investigation on model surfaces. *J. Adhes. Sci. Technol.* **24**, 2141–2164. (doi:10.1163/016942410X507966)
43. Katz BZ, Yamada KM. 1997 Integrins in morphogenesis and signaling. *Biochemie* **79**, 467–476. (doi:10.1016/S0300-9084(97)82738-1)
44. Timpl R, Brown JC. 1994 The laminins. *Matrix. Biol.* **14**, 75–81. (doi:10.1016/0945-053X(94)90192-9)
45. Sudhakaran PR, Viji RI, Kiran MS, Sameer Kumar VB. 2009 Endothelial cell–laminin interaction: modulation of LDH expression involves $\alpha 6\beta 4$ integrin-FAK-p38MAPK pathway. *Glycoconj. J.* **26**, 697–704. (doi:10.1007/s10719-008-9188-7)
46. Sonnenberg A, Linders CJT, Modderman PW, Damsky CH, Aumailley M, Timpl R. 1990 Integrin recognition of different cell binding fragments of laminin (PI, E3, E8) and evidence that $\alpha 6\beta 1$ but not $\alpha 6\beta 4$ functions as a major receptor for fragment E8. *J. Cell. Biol.* **110**, 2145–2155. (doi:10.1083/jcb.110.6.2145)
47. Pratt KJ, Jarrell BE, Williams SK, Carabasi RA, Rupnick MA, Hubbard FA. 1988 Kinetics of endothelial cell-surface attachment forces. *J. Vasc. Surg.* **7**, 591–599. (doi:10.1067/mva.1988.avs0070591)